Super-Resolution TOA Estimation With Diversity for Indoor Geolocation

Xinrong Li, *Student Member, IEEE,* and Kaveh Pahlavan, *Fellow, IEEE*

***Abstract*—This paper presents an in-depth investigation of frequency-domain super-resolution time-of-arrival (TOA) estimation with diversity techniques for indoor geolocation applications. A methodology for performance evaluation of super-resolution techniques based on the measurements of indoor radio propagation channels is presented. The performance of super-resolution techniques is compared with the performance of conventional TOA estimation techniques. The effects of diversity techniques on the performance of super-resolution techniques are evaluated. The measurement and simulation methods presented in this paper can be used to establish empirical performance bounds for real implementation of super-resolution indoor geolocation systems.**

***Index Terms*—Channel measurement, diversity techniques, indoor geolocation, performance evaluation, spectrum estimation, super-resolution, time-of-arrival (TOA) estimation.**

I. Introduction

With the emergence of location-based applications and next-generation location-aware wireless networks, location finding techniques are becoming increasingly important [1]. Location finding based on time-of-arrival (TOA) is the most popular method for accurate positioning systems. The basic problem in TOA-based techniques is to accurately estimate the propagation delay of the radio signal arriving from the direct line-of-sight (DLOS) propagation path. However, in indoor and urban areas, due to severe multipath conditions and the complexity of the radio propagation, the DLOS cannot always be accurately detected [2], [3]. Increasing time-domain resolution of channel response to resolve the DLOS path improves the performance of location finding systems employing TOA estimation techniques.

Super-resolution techniques have been studied in the field of spectral estimation [4]. Recently, a number of researchers have applied super-resolution spectral estimation techniques for time-domain analysis of different applications. These applications include electronic devices parameter measurement [5], [6] and multipath radio propagation studies [7]–[11]. In [7], the super-resolution technique was employed in the frequency domain to estimate multipath time dispersion parameters such as mean excess delay and root-mean-square delay spread. A similar method was used in [8] to model indoor radio propagation channels with parametric harmonic signal models. Here, we address the application of super-resolution techniques to accurate TOA estimation for indoor geolocation. In the literature, the time-delay estimation problem has been studied with a variety of super-resolution techniques, such as minimum-norm [9], root multiple signal classification (MUSIC) [10], and total least square-estimation of signal parameters via rotational invariance techniques (TLS-ESPRIT) [11]. While super-resolution techniques can increase time-domain resolution, it also increases complexity of system implementation. In this paper, we present an investigation of frequency-domain super-resolution TOA estimation techniques for indoor geolocation. We present and evaluate techniques that can be used in practical implementation to improve the performance of TOA estimation. To demonstrate usefulness, the performance of super-resolution techniques is compared with that of two conventional TOA estimation techniques. In addition, two diversity combining schemes are presented for super-resolution TOA estimation techniques and the effects of diversity techniques are evaluated based on these two schemes.

In the literature, the performance of super-resolution techniques for time-domain analysis is typically evaluated either by computer simulation with simple two-path channel model [9] or by using specially designed simple circuits [6]. In this paper, the performance of super-resolution TOA estimation techniques is studied through computer simulations based on measurements of indoor radio propagation channels. Due to the complexity of multipath indoor radio channels, performance analysis based on experimental channel measurement data reveals much more realistic statistical results than computer simulations with simple theoretical channel models. Furthermore, as the channel measurement system that we used provides a convenient means for conducting extensive measurements in indoor areas, the measurement and simulation methods presented in this paper can be used to conveniently establish empirical performance bounds for real implementation of super-resolution indoor geolocation systems.

The rest of the paper is organized as follows. In Section II, the MUSIC super-resolution algorithm is applied to the frequency-domain channel measurement data for TOA estimation. Then several issues in practical implementation are addressed in Section III. Section IV presents diversity techniques that can be applied to super-resolution TOA estimation. Simulation results based on measurement data are presented in Section V, which is followed by conclusions.

Manuscript received December 8, 2001; revised July 2, 2002; accepted October 4, 2002. The editor coordinating the review of this paper and approving it for publication is K. B. Lee. This work was supported in part by the National Science Foundation under Grant ECS-0084112.

The authors are with the Department of Electrical and Computer Engineering, Worcester Polytechnic Institute, Worcester, MA 01609 USA (e-mail: xinrong@wpi.edu; kaveh@wpi.edu).

Digital Object Identifier 10.1109/TWC.2003.819035

II. Super-Resolution Techniques

The multipath indoor radio propagation channel is normally modeled as a complex lowpass equivalent impulse response given by

$$h(t) = \sum_{k=0}^{L_p-1} \alpha_k \delta(t - \tau_k) \tag{1}$$

where L_p is the number of multipath components, and $\alpha_k = |\alpha_k| e^{j\theta_k}$ and τ_k are the complex attenuation and propagation delay of the kth path, respectively, while the multipath components are indexed so that the propagation delays τ_k, $0 \le k \le L_p - 1$ are in ascending order. As a result, τ_0 in the model denotes the propagation delay of the DLOS path, i.e., the TOA, which needs to be detected for the purpose of indoor geolocation. Taking the Fourier transform of (1), the frequency-domain channel response can be expressed as

$$H(f) = \sum_{k=0}^{L_p-1} \alpha_k e^{-j2\pi f \tau_k}. \tag{2}$$

The parameters α_k and τ_k are random time-variant functions because of the motion of people and equipment in and around buildings. However, since the rate of their variations is very slow as compared with the measurement time interval, these parameters can be treated as time-invariant random variables within one snapshot of measurement [12]. The phase of the complex attenuation θ_k is normally assumed random from one snapshot to another with a uniform probability density function $U(0, 2\pi)$ [13]. On the other hand, these parameters are frequency-dependent since they are related to radio signal characteristics such as transmission and reflection coefficients. However, as shown in [14], for frequency bands used in this paper, these parameters can be assumed frequency-independent.

In this paper, we consider super-resolution TOA estimation based on frequency-domain measurement of indoor channel response. In practice, discrete samples of frequency-domain channel response can be obtained by sweeping the channel at different frequencies [15], by using a multicarrier modulation technique such as orthogonal frequency-division multiplexing (OFDM), or in a direct-sequence spread spectrum (DSSS) system by deconvolving the received signal over the frequency band of high signal-to-noise ratio [7], [9]–[11].

If we exchange the role of time and frequency variables in (2), we can observe that it becomes a harmonic signal model

$$H(\tau) = \sum_{k=0}^{L_p-1} \alpha_k e^{-j2\pi f_k \tau} \tag{3}$$

which is well known in spectral estimation field [4]. Consequently, any spectral estimation techniques that are suitable for the harmonic signal model can be applied to the frequency response of multipath indoor radio channel to perform time-domain analysis. In this paper, we use the MUSIC algorithm [16], as an example of super-resolution techniques, in TOA estimation for indoor geolocation applications.

The discrete measurement data are obtained by sampling channel frequency response $H(f)$ at L equally spaced frequencies. Considering additive white noise in the measurement process, the sampled discrete frequency-domain channel response is given by

$$x(l) = H(f_l) + w(l) = \sum_{k=0}^{L_p-1} \alpha_k e^{-j2\pi(f_0 + l\Delta f)\tau_k} + w(l) \tag{4}$$

where $l = 0, 1, \ldots, L-1$, and $w(l)$ denotes additive white measurement noise with mean zero and variance σ_w^2. We can then write this signal model in vector form

$$\mathbf{x} = \mathbf{H} + \mathbf{w} = \mathbf{V}\mathbf{a} + \mathbf{w} \tag{5}$$

where

$$\begin{aligned}
\mathbf{x} &= [\,x(0) \quad x(1) \quad \ldots \quad x(L-1)\,]^T \\
\mathbf{H} &= [\,H(f_0) \quad H(f_1) \quad \ldots \quad H(f_{L-1})\,]^T \\
\mathbf{w} &= [\,w(0) \quad w(1) \quad \ldots \quad w(L-1)\,]^T \\
\mathbf{V} &= [\,\mathbf{v}(\tau_0) \quad \mathbf{v}(\tau_1) \quad \ldots \quad \mathbf{v}(\tau_{L_p-1})\,] \\
\mathbf{v}(\tau_k) &= [\,1 \quad e^{-j2\pi\Delta f \tau_k} \quad \ldots \quad e^{-j2\pi(L-1)\Delta f \tau_k}\,]^T \\
\mathbf{a} &= [\,\alpha'_0 \quad \alpha'_1 \quad \ldots \quad \alpha'_{L_p-1}\,]^T \\
\alpha'_k &= \alpha_k e^{-j2\pi f_0 \tau_k}
\end{aligned}$$

and the superscript T denotes the matrix transpose operation.

The MUSIC super-resolution techniques are based on eigendecomposition of the autocorrelation matrix of the preceding signal model in (5)

$$\mathbf{R}_{xx} = E\{\mathbf{x}\mathbf{x}^H\} = \mathbf{V}\mathbf{A}\mathbf{V}^H + \sigma_w^2 \mathbf{I} \tag{6}$$

where $\mathbf{A} = E\{\mathbf{a}\mathbf{a}^H\}$ and the superscript H denotes conjugate transpose operation, i.e., Hermitian, of a matrix. Since the propagation delays τ_k in (1) can be theorectically assumed all different, and the matrix $\mathbf{V}$ has full column rank, i.e., the column vectors of $\mathbf{V}$ are linearly independent. If we assume the magnitude of the parameters α_k is constant and the phase is a uniform random variable in $[0, 2\pi]$, the $L_p \times L_p$ covariance matrix $\mathbf{A}$ is nonsingular. Then, from the theory of linear algebra, it follows that assuming $L > L_p$, the rank of the matrix $\mathbf{V}\mathbf{A}\mathbf{V}^H$ is L_p, or equivalently, the $L - L_p$ smallest eigenvalues of $\mathbf{R}_{xx}$ are all equal to σ_w^2. The eigenvectors (EVs) corresponding to $L - L_p$ smallest eigenvalues of $\mathbf{R}_{xx}$ are called noise EVs, while the EVs corresponding to L_p largest eigenvalues are called signal EVs. Thus, the L-dimensional subspace that contains the signal vector $\mathbf{x}$ can be split into two orthogonal subspaces, known as signal subspace and noise subspace, by the signal EVs and noise EVs, respectively. The projection matrix of the noise subspace is then determined by

$$\mathbf{P}_w = \mathbf{Q}_w (\mathbf{Q}_w^H \mathbf{Q}_w)^{-1} \mathbf{Q}_w^H = \mathbf{Q}_w \mathbf{Q}_w^H \tag{7}$$

where $\mathbf{Q}_w = [\,\mathbf{q}_{L_p} \quad \mathbf{q}_{L_p+1} \quad \ldots \quad \mathbf{q}_{L-1}\,]$ and $\mathbf{q}_k$, $L_p \le k \le L-1$ are noise EVs. Since the vector $\mathbf{v}(\tau_k)$, $0 \le k \le L_p - 1$ must lie in the signal subspace, we have

$$\mathbf{P}_w \mathbf{v}(\tau_k) = 0. \tag{8}$$

Thus, the multipath delays τ_k, $0 \le k \le L_p - 1$ can be determined by finding the delay values at which the following MUSIC pseudospectrum achieves maximum value:

$$\begin{aligned}
S_{\mathrm{MUSIC}}(\tau) &= \frac{1}{||\mathbf{P}_w \mathbf{v}(\tau)||^2} = \frac{1}{\mathbf{v}^H(\tau)\mathbf{P}_w\mathbf{v}(\tau)} = \frac{1}{||\mathbf{Q}_w^H \mathbf{v}(\tau)||^2} \\
&= \frac{1}{\sum_{k=L_p}^{L-1} |\mathbf{q}_k^H \mathbf{v}(\tau)|^2}.
\end{aligned} \tag{9}$$

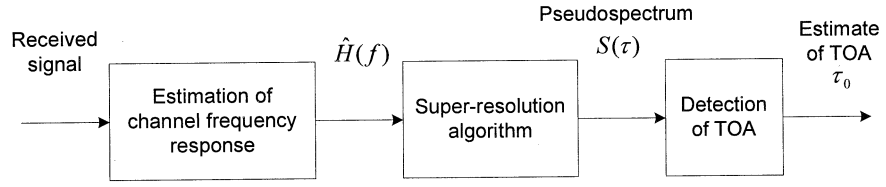

Fig. 1. Functional block diagram of the receiver of super-resolution TOA estimation systems.

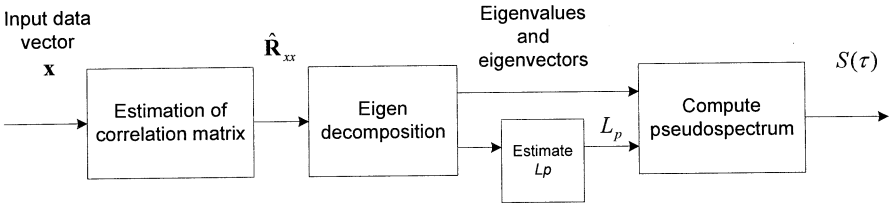

Fig. 2. Functional block diagram of the MUSIC super-resolution TOA estimation algorithm.

Fig. 1 shows a functional block diagram of the receiver of super-resolution TOA estimation systems. The received signal is first used to estimate channel frequency response. Then, a super-resolution algorithm is used to transform the channel frequency response to time domain pseudospectrum, as defined in (9). The estimate of TOA is then obtained by detecting the first peak of the pseudospectrum in the delay axis using a peak detection algorithm. In the next section, issues in the practical implementation of super-resolution TOA estimation techniques will be presented.

III. Issues in Practical Implementation

Note that in the analysis, we considered the theoretical or true correlation matrix $\mathbf{R}_{xx}$. In practice, the correlation matrix must be estimated from the measured data samples. Fig. 2 illustrates a functional block diagram of the MUSIC super-resolution TOA estimation algorithm. The input data vector, i.e., the estimate of channel frequency response given in (5), is first used to estimate the correlation matrix $\mathbf{R}_{xx}$. Then, the eigenvalues as well as the corresponding EVs of the correlation matrix are computed. The parameter L_p is determined through the analysis of the eigenvalues and EVs of the correlation matrix, which is discussed in details later in this section. Finally, the pseudospectrum is obtained using (9).

If we have P snapshots of measurement data, the estimate of the correlation matrix is obtained from

$$\hat{\mathbf{R}}_{xx} = \frac{1}{P}\sum_{k=1}^{P}\mathbf{x}^{(k)}\mathbf{x}^{(k)H} \tag{10}$$

but if only one snapshot of measurement data of length N is available, the data sequence is divided into M consecutive segments of length L and then the correlation matrix is estimated as

$$\hat{\mathbf{R}}_{xx} = \frac{1}{M}\sum_{k=0}^{M-1}\mathbf{x}(k)\mathbf{x}(k)^{H} \tag{11}$$

where $M = N - L + 1$ and $\mathbf{x}(k) = [x(k) \quad \dots \quad x(k+L-1)]^T$. In this section, we will focus on the second method, where only one snapshot of measurement data is used in estimating data correlation matrix as in (11). Methods based on multiple snapshots will be discussed in Section IV for application with diversity techniques.

As we mentioned earlier, for the super-resolution TOA estimation techniques, the measurement data vector $\mathbf{x}$ is obtained by sampling channel frequency response uniformly over a given frequency band. In order to avoid aliasing in the time domain, similar to the time-domain Nyquist sampling theorem, the frequency-domain sampling interval Δf is determined to satisfy the condition $1/\Delta f \geq 2\tau_{\max}$, where $\tau_{\max} = \max(\tau_{L_p-1})$ is the maximum delay of the measured multipath radio propagation channel. For example, for indoor geolocation applications, the frequency sampling interval Δf is normally set to be 1 MHz, which accommodates application scenarios where the maximum delay $\tau_{\max}$ is less than 500 ns or, equivalently, the maximum length of the multipath signal propagation path is less than 150 m. Thus, with a bandwidth of 20 MHz, the length of one measurement data sequence is 21, which is far too short to accurately estimate the correlation matrix. As we will discuss, a number of issues arise and a number of techniques can be used to improve the performance when the estimate of the correlation matrix is used in the implementation of super-resolution techniques.

A. Improved Estimation of Correlation Matrix With Limited Measurement Data

The measurement data are assumed to be stationary. Thus, the correlation matrix of the data is Hermitian (conjugate symmetric) and Toeplitz (equal elements along all diagonals). However, the estimate of the correlation matrix $\hat{\mathbf{R}}_{xx}$, based on the actual measurement data of small finite length N, is not Toeplitz. The estimate of the correlation matrix can be improved using the following *forward–backward correlation matrix* (FBCM):

$$\hat{\mathbf{R}}_{xx}^{(\mathrm{FB})} = \frac{1}{2}(\hat{\mathbf{R}}_{xx} + \mathbf{J}\hat{\mathbf{R}}_{xx}^{*}\mathbf{J}) \tag{12}$$

where the superscript $*$ denotes conjugate, superscript FB stands for forward–backward estimation, and $\mathbf{J}$ is the $L \times L$ exchange matrix whose components are zero except for ones on the antidiagonal. It can be easily shown that $\hat{\mathbf{R}}_{xx}^{(\mathrm{FB})}$ is persymmetric, that is, $\mathbf{J}\hat{\mathbf{R}}_{xx}^{(\mathrm{FB})}\mathbf{J} = \hat{\mathbf{R}}_{xx}^{(\mathrm{FB})*}$, and its elements

are conjugate symmetric about both main diagonals. This technique is widely used in spectral estimation with the name *modified covariance method* [4], in linear least-square signal estimation with the name *forward–backward linear predication* [4], and in antenna array signal processing with the name *modified spatial smoothing preprocessing* [6], [17]. Here, we call the correlation matrix in (11) the *forward correlation matrix* (FCM) in contrast to the FBCM in (12).

In our development of basic theories, we assumed that the magnitude of the parameters α_k in (1) is constant and the phase θ_k is a uniformly distributed random variable so that the correlation matrix $\mathbf{A}$ in (6) is full-rank (nonsingular), but if the phase of α_k is nonrandom, which is true if only one snapshot of measurement data is used in estimating the correlation matrix $\mathbf{R}_{xx}$, the rank of the correlation matrix $\mathbf{A}$ decreases to one and the matrix becomes singular. In such a situation, the MUSIC algorithm does not work properly, but fortunately, for the signal model (4), the estimation of data correlation matrix using (11) has decorrelation effects. The decorrelation effects in forward and forward–backward correlation matrices were analyzed in [6], [17], and [18]. For the forward estimation method, following the derivation in [18] for the two-source model, the correlation coefficient between α_i' and α_j', i.e., the ith and jth element of $\mathbf{a}$, can be derived as

$$\rho_{ij}^{(\mathrm{FCM})} = \frac{A_{ij}}{\sqrt{A_{ii}A_{jj}}} = Ke^{-j\phi} \tag{13}$$

where

$$K = \frac{\sin[M\pi\Delta f(\tau_i - \tau_j)]}{M\sin[\pi\Delta f(\tau_i - \tau_j)]}$$
$$\phi = -(\theta_i - \theta_j) + 2\pi f_0(\tau_i - \tau_j) + \pi(M-1)\Delta f(\tau_i - \tau_j)$$

and A_{ij} is the (i,j)th element of the parameter correlation matrix $\mathbf{A}$. It is noted that the decorrelation effects of the forward estimation method depend on the number of segments M, the frequency sampling interval Δf, and time-delay difference $(\tau_i - \tau_j)$. Similarly, the correlation coefficient of the forward–backward estimation method can be derived as

$$\rho_{ij}^{(\mathrm{FBCM})} = K\cos\left(\phi + \frac{\psi}{2}\right)e^{j\psi/2} \tag{14}$$

where

$$\psi = 2\pi(L-1)\Delta f(\tau_i - \tau_j)$$

which depends, in addition, on the length of the segments L, phase difference of parameters $(\theta_i - \theta_j)$, and the lowest frequency of the spectrum f_0. Detailed derivations of (13) and (14) can be found in the Appendix. From

$$\left|\rho_{ij}^{(\mathrm{FBCM})}\right| = \left|\rho_{ij}^{(\mathrm{FCM})}\right| \times \left|\cos\left(\phi + \frac{\psi}{2}\right)\right| \tag{15}$$

we can clearly observe that FBCM has better decorrelation effects than the FCM. Fig. 3 shows examples of the decorrelation effects versus the number of segments calculated from (13) and (14), respectively. Later in this paper, we compare the performance of the forward and forward–backward estimation methods by computer simulations.

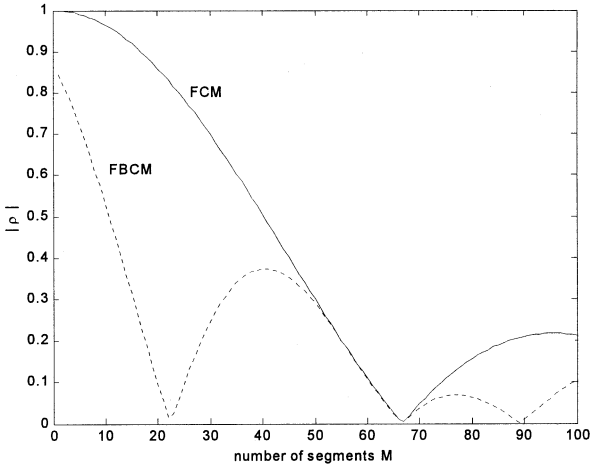

Fig. 3. Correlation coefficients of FCM and FBCM, with $\Delta f = 1$ MHz, $(\tau_i - \tau_j) = 15$ ns, $(\theta_i - \theta_j) = 0$, $f_0 = 900$ MHz, and $L = 13$.

B. Determination of Parameters L and L_p

If we use only one measurement data snapshot of length N points to estimate the TOA, the first step is to determine the value of L for estimation of $\hat{\mathbf{R}}_{xx}$ as in (11). With large values of L, the potential for higher resolution of the MUSIC algorithm increases, which is similar to that in array signal processing where increasing L means an increase in subarray aperture and, thus, an increase in resolution capability [19], [20]. On the other hand, from (11), we can see that for a fixed value of N, the value of M decreases as L increases. The decrease in M increases fluctuations in the matrix $\hat{\mathbf{R}}_{xx}$, resulting in large perturbations of the eigenvalues and EVs of $\mathbf{R}_{xx}$, and reduces the number of coherent α_k that can be detected [20], [21]. Consequently, the value of L needs to be selected so that it provides a balance between resolution and stability of the algorithm. Different values of L have been used in the literature; for example, [22] used $N/2$ and $N/3$, [19] used $3N/4$, and [9] adopted $3N/5$. In this paper, we use a value of $2N/3$, which was determined through computer simulations.

Another parameter that needs to be determined in using a super-resolution technique is the number of multipath components L_p. If the true correlation matrix $\mathbf{R}_{xx}$ is available, L_p can be easily determined by observing eigenvalues of the correlation matrix since in theory, the $L - L_p$ smallest eigenvalues of $\mathbf{R}_{xx}$ are all equal to σ_w^2, and the remaining L_p eigenvalues are all larger than σ_w^2, but in practical implementation, especially when the correlation matrix is estimated from a limited number of data samples, the noise eigenvalues are all different, which makes it challenging to clearly distinguish signal eigenvalues and noise eigenvalues. In [23], the information theoretic criteria for model selection, including Akaike information theoretic criteria and Rissanen minimum descriptive length criteria (MDL), are applied to this problem. The MDL criterion for estimation of L_p is used in this paper, which is given as [23]

$$\mathrm{MDL}(k) = -\log\left(\frac{\prod_{i=k}^{L-1}\lambda_i^{1/(L-k)}}{\frac{1}{L-k}\sum_{i=k}^{L-1}\lambda_i}\right)^{M(L-k)} + \frac{1}{2}k(2L-k)\log M \tag{16}$$

where λ_i, $0 \le i \le L-1$ are the eigenvalues of correlation matrix in descending order. The estimate of L_p is determined as the value of $k \in [0, L-1]$ for which the MDL is minimized. In [24], Xu *et al.* showed that when the forward–backward estimation method is used, the MDL criteria in (16) cannot directly apply and the second term of the criteria must be modified to $(1/4)k(2L-k+1)\log M$.

C. EV Method

One implicit assumption in the MUSIC method is that the noise eigenvalues are all equal, i.e., $\lambda_k = \sigma_w^2$ for $L_p \le k \le L-1$, that is, the noise is white. However, as we just discussed, when the correlation matrix is estimated from a limited number of data samples in practice, the noise eigenvalues are not equal. A slight variation on the MUSIC algorithm, known as the EV method, can be used to account for the potentially different noise eigenvalues [4], [25]. The pseudospectrum of the EV algorithm is defined as

$$S_{\mathrm{EV}}(\tau) = \frac{1}{\sum_{k=L_p}^{L-1} \frac{1}{\lambda_k} |\mathbf{q}_k^H \mathbf{v}(\tau)|^2} \tag{17}$$

where λ_k, $L_p \le k \le L-1$ are the noise eigenvalues. In effect, the pseudospectrum of each EV is normalized by its corresponding eigenvalue. If the noise eigenvalues are equal, the EV method and the MUSIC method are identical. The performance of the MUSIC and EV methods were compared in [25], and it was shown that the EV method is less sensitive to inaccurate estimate of the parameter L_p, which is highly desirable in a practical implementation. As presented later in this paper, the EV method is shown by computer simulations to have slightly better performance than the MUSIC method. In Section IV, we investigate diversity techniques that can be used to further improve the performance of super-resolution TOA estimation techniques.

IV. Diversity Techniques

Diversity techniques such as time diversity, space diversity, and frequency diversity are widely utilized in wireless communication systems to improve link performance [1], [13], [26]. Diversity techniques take advantage of the random nature of the radio propagation channel by finding and combining uncorrelated signal paths. In essence, all diversity techniques used for wireless communication systems can be used for TOA estimation systems with the general structure shown in Fig. 4, where the diversity system has P branches. The TOA is estimated independently at each diversity branch of receiver, and then a combining algorithm is used to process the TOA estimates from all branches to obtain an optimum estimate. A variety of different combining algorithms can be designed for different diversity techniques. The simplest one is the equal-gain combining algorithm given by

$$\hat{\tau}_0 = \frac{1}{P} \sum_{k=1}^{P} \hat{\tau}_0^{(k)}. \tag{18}$$

In some cases, more complex variable-gain combining is also possible, where the estimate of each diversity branch

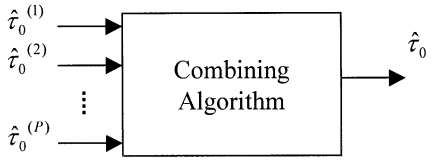

Fig. 4. General structure of TOA estimation with diversity techniques.

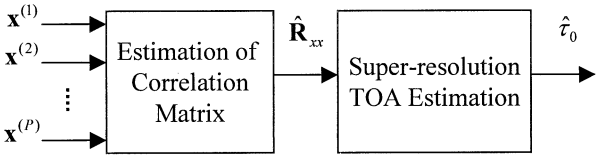

Fig. 5. Estimation of correlation matrix with diversity techniques for super-resolution TOA estimation, correlation matrix based diversity combining scheme (CMDCS).

is weighted with a coefficient that reflects the quality of time-delay estimation at each branch. More research work is needed to design optimum combining algorithms for diversity techniques.

For the super-resolution TOA estimation techniques presented in this paper, diversity techniques can also be applied, as shown in Fig. 5. Instead of combining independent time-delay estimates as in Fig. 4, the measurement data at diversity branches are combined to estimate the correlation matrix using (10). For the convenience of referencing, we call the structure in Fig. 4(a) the *general diversity combing scheme* (GDCS), and the structure in Fig. 5(a), the *correlation matrix-based* diversity combing scheme (CMDCS). In super-resolution TOA estimation techniques, the major computational load is in the eigen analysis, i.e., computing eigenvalues and EVs, of the correlation matrix. As a result, CMDCS is computationally superior to GDCS since the CMDCS scheme performs eigen analysis only once, but the GDCS scheme needs to perform independent eigen analysis P times.

On the other hand, by applying the CMDCS scheme, the underlying assumption concerning the radio propagation channel is that the amplitude attenuation and time delay for each path, and the number of signal paths are the same from the transmitter to all diversity branches of the receiver. This restricts CMDCS to only quasistationary scenarios, where the channel remains unchanged while the P diversity measurement data are collected. This is one disadvantage of the CMDCS scheme as compared with the GDCS scheme, which has no such restriction in application. This condition for applicability also makes it challenging to use CMDCS for space diversity since in space-diversity situations, the radio propagation channel from the transmitter to diversity branches of the receiver are most likely not the same. Similarly, CMDCS is not suitable for time diversity. As we discussed in Section III, the super-resolution technique cannot work properly when the phase of each signal path remains unchanged together with the amplitude attenuation and time delay for each path, and the number of signal paths. For quasistationary scenarios, it is unknown whether the phase is random or not for repeated measurements while the number of signal paths and the amplitude attenuation and time delay for each path all remain unchanged, but simulation results utilizing

measurement data collected on indoor radio channels, which will be presented in Section V, show that time-diversity with CMDCS yield almost no improvement over nondiversity techniques. In contrast, frequency-diversity can be well fitted into CMDCS. By using frequency-diversity, the kth measurement data vector $\mathbf{x}^{(k)}$, $1 \le k \le P$ are obtained using kth carrier frequency. A quantitative relationship between the improvement of TOA estimation accuracy and frequency diversity is not known, but the effects of frequency diversity can be conveniently analyzed using the correlation coefficients similar to the way by which we analyzed the forward–backward correlation method.

For frequency diversity, if the carrier frequency f_0 is uniformly distributed

$$f_0 \sim U\left(f_c - \frac{\Delta F}{2}, f_c + \frac{\Delta F}{2}\right) \tag{19}$$

where f_c is center frequency, and ΔF is the range of the frequency distribution, the correlation coefficient between α_i' and α_j' can be derived as

$$\rho_{ij}^{(\mathrm{FD})} = \frac{\sin(\pi\Delta F(\tau_i - \tau_j))}{\pi\Delta F(\tau_i - \tau_j)} e^{j[(\theta_i - \theta_j) - 2\pi f_c(\tau_i - \tau_j)]} \tag{20}$$

where the superscript FD stands for frequency diversity. Similarly, if the frequency diversity method is used for the FCM, then the correlation coefficient becomes

$$\rho_{ij}^{(\mathrm{FCM,FD})} = K' e^{-j\phi'} \tag{21}$$

where

$$K' = K\frac{\sin(\pi\Delta F(\tau_i - \tau_j))}{\pi\Delta F(\tau_i - \tau_j)}$$
$$\phi' = -(\theta_i - \theta_j) + 2\pi f_c(\tau_i - \tau_j) + \pi(M-1)\Delta f(\tau_i - \tau_j)$$

and that for FBCM becomes

$$\rho_{ij}^{(\mathrm{FBCM,FD})} = K' \cos\left(\phi' + \frac{\psi}{2}\right) e^{j\psi/2}. \tag{22}$$

We notice that by using the frequency diversity method, the coherence between multipath components is decorrelated according to the *sinc* finction as ΔF and absolute value of delay difference $(\tau_i - \tau_j)$ increase. Fig. 6 shows correlation coefficients of forward and forward–backward correlation matrices with frequency diversity, calculated from (21) and (22), using the same parameters as in Fig. 3. We can clearly observe that the frequency diversity technique further improves the decorrelation effects in both forward and forward–backward correlation matrices. Details of the derivations of (20)–(22) are presented in the Appendix.

V. Simulation Results Based on Measurement Data

In this section, we further investigate the performance of super-resolution and diversity techniques by means of computer simulations based on the measured frequency response of indoor radio propagation channels. The frequency response of the indoor radio channel can be measured with a network analyzer, as reported in [15] and [27]. The main component of our measurement system is a network analyzer that generates a swept frequency signal and analyzes the resulting received signal. The measurement data reported in [28], collected using a network analyzer, is used in this paper to evaluate the performance of super-resolution TOA estimation techniques. Magnitude and phase measurements of radio channels were performed at center frequency 1 GHz with bandwidth of 200 MHz. The measurements were conducted at three different buildings that represent highly likely places for deployment of indoor geolocation systems, including a manufacturing building at the Norton Company, Worcester, MA, a modern academic building, the Fuller Laboratory at Worcester Polytechnic Institute, Worcester, MA, and a residential house, the Schussler House at Worcester Polytechnic Institute. Thirty locations were selected at each site for measurement at places where indoor geolocation systems will be likely used. Four consecutive snapshots of the radio channel were taken at each receiver location while preventing movement around the vicinity of the antennas of transmitter and receiver. During the measurement, a transmitter was fixed at one location while a receiver was moved around. The measurement locations were distributed so as to include indoor-to-indoor, outdoor-to-indoor, and outdoor-to-second floor radio propagation conditions. For each measurement location, the physical distance between the antennas of transmitter and receiver were determined either directly or from the blueprint of building floorplans. After the measurement, the frequency domain measurement data were calibrated to remove the effects of system and antenna gains and delays [15].

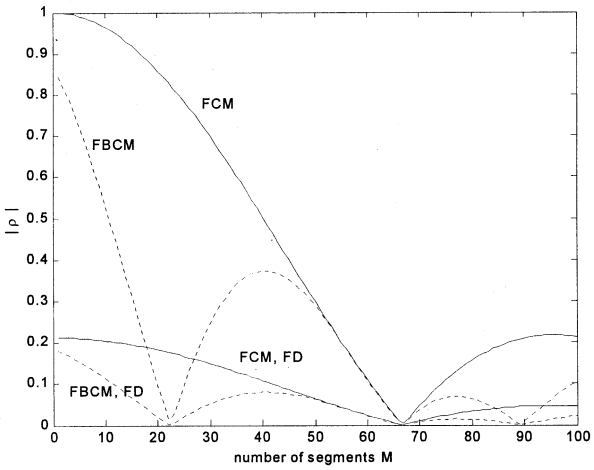

Fig. 6. Correlation coefficients of FCM and FBCM with and without frequency diversity, with $\Delta f = 1$ MHz, $(\tau_i - \tau_j) = 15$ ns, $(\theta_i - \theta_j) = 0$, $f_c = 1$ GHz, $L = 13$, and $\Delta F = 100$ MHz.

The signal bandwidth is one of the key factors affecting the accuracy of TOA estimation in multipath propagation environments [3]. To study the performance of TOA estimation using signals of various bandwidths, in the simulations, we use only a segment of each frequency domain measurement data to reflect the band-limitation effects. For example, with a 1-MHz frequency-domain sampling interval, a data segment of 21 samples, centered at 1 GHz, of each measurement data is used in simulations for a bandwidth of 20 MHz.

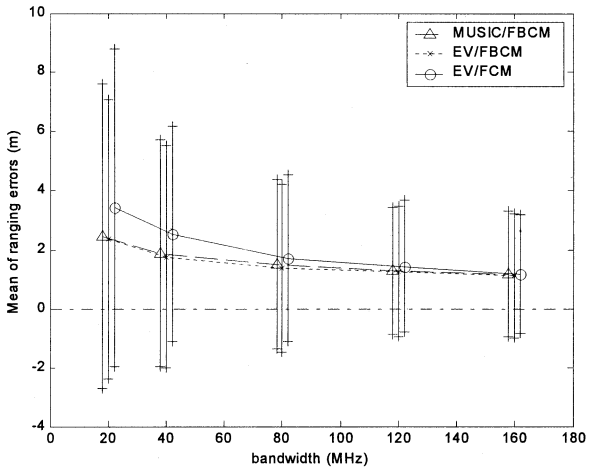

Fig. 7. Mean and STD of ranging errors using different techniques. The vertical line corresponds to plus and minus one STD about the mean.

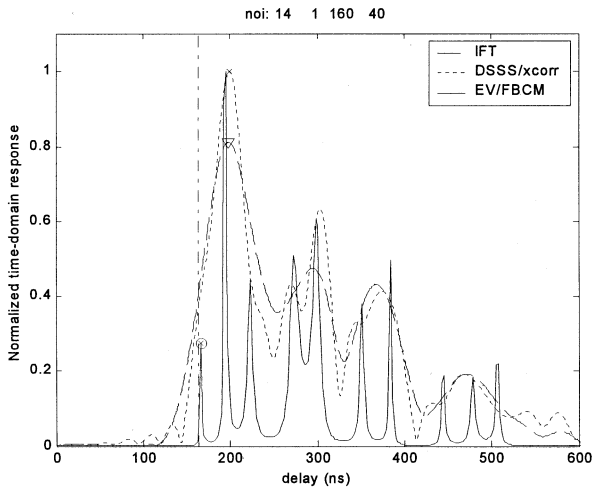

Fig. 8. Estimated TOA of the DLOS path and normalized time-domain responses obtained using three different techniques. The vertical dashed–dotted line denotes the expected TOA.

A. Performance of Super-Resolution Techniques

As we mentioned earlier, the EV method is a variant of the MUSIC method and it is preferred when the correlation matrix is estimated from a limited number of data samples. To compare the performance of EV and MUSIC methods, both algorithms are applied to the measured data with forward–backward estimation of the correlation matrix. Fig. 7 presents the mean and standard deviation (STD) of the ranging errors versus signal bandwidth. To clearly relate the results to geolocation applications, time delay τ is converted to distance d by the relationship $d = c \times \tau$, where $c = 3 \times 10^8$ m/s is the constant speed of light in free space. We can observe that both mean and STD of the ranging errors decrease as the bandwidth increases. The EV method (i.e., EV/FBCM) has slightly better performance than the MUSIC (i.e., MUSIC/FBCM) for low signal bandwidth in terms of smaller STD of ranging errors. As a result, in the following, we use the EV algorithm for further investigation.

We analyzed FCM-based and FBCM-based super-resolution TOA estimation techniques through the decorrelation effects in the estimated correlation matrix. Since there is no analytical way to quantitatively relate the improvement in the accuracy of TOA estimation to the method of correlation matrix estimation, we compare the two methods using statistical simulation results. Fig. 7 also presents simulation results for the EV algorithm with FCM. Comparing EV/FBCM and EV/FCM, it is clear that the FBCM-based method performs better than the FCM-based method in terms of smaller mean and STD of ranging errors, which is consistent with the analytical analysis. It is also noted that both techniques have similar performance when the signal bandwidth is large, e.g., bandwidth larger than 120 MHz.

B. Comparison of Super-Resolution and Conventional Techniques

In order to demonstrate the usefulness of the super-resolution technique, we compare its performance with two conventional time-delay estimation techniques. In the first of the other two techniques, the frequency-domain channel response is converted directly to time domain using the inverse Fourier transform (IFT), and then, propagation delay of the DLOS is detected. When the time-domain response over part of the time period is desired, the chirp-z transform (CZT) is preferred, providing flexibility in the choice of time-domain parameters with the cost of longer computational time as compared with IFFT (inverse fast Fourier transform) [29]. The time-domain resolution with CZT is the same as with the IFFT. On the other hand, a proper window function is needed to avoid leakage and false peaks by reducing the sidelobes of the time-domain response, which result from finite bandwidth, with the cost of reduced time-domain resolution. In our simulations, we employ CZT with the Hanning window to convert frequency channel response to the time domain.

The second technique uses the traditional cross-correlation techniques with DSSS signals (DSSS/xcorr). To simulate DSSS signal-based cross-correlation technique using measured frequency channel response data, frequency response of a raised-cosine pulse with rolloff factor 0.25 is first applied to the frequency channel response as a combined response of band-limitation pulse-shaping filters of the transmitter and receiver. Then, the resultant frequency response is converted to the time domain using the IFT for TOA estimation.

Fig. 8 shows normalized time-domain responses obtained from simulations of the three techniques using a sample channel measurement data. We observe that the super-resolution technique shows much higher time-domain resolution than the other two, and it accurately detects the delay of the DLOS path while the other two fail. Fig. 9(a) presents mean and STD of ranging errors versus the bandwidth of the system. Fig. 9(b) presents probabilities of measurement locations where absolute ranging errors are smaller than 3 m. In general, the super-resolution technique has the best performance and it is preferred, especially when the signal bandwidth is small. It should be noted that, as shown in the simulation results, while using super-resolution technique and larger bandwidth can improve the statistical performance of TOA estimation, it cannot eliminate large estimation errors at some locations. This is because of the possibility of no-LOS propagation (NLOS)

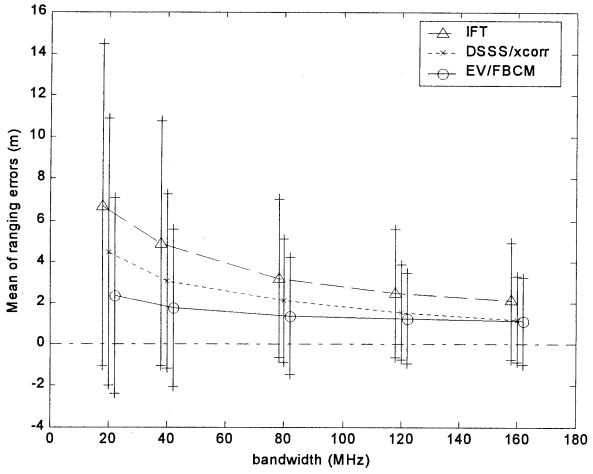

(a)

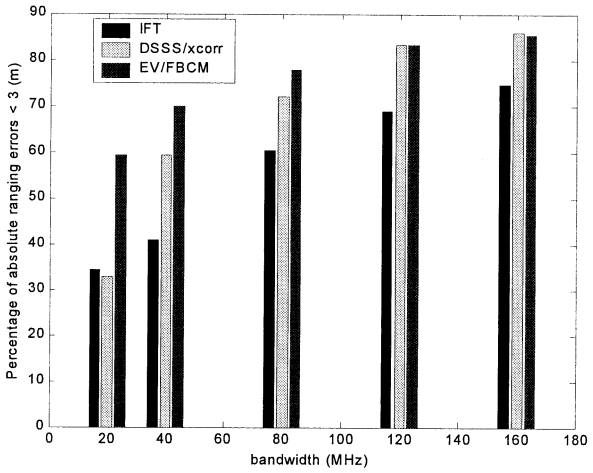

(b)

Fig. 9. Simulation results. (a) Mean of ranging errors using three different TOA estimation techniques. The vertical line corresponds to one STD. (b) Percentages of measurement locations where absolute ranging errors are smaller than 3 m.

condition between the transmitter and the receiver. Such a condition needs to be dealt with in the positioning process to achieve high positional accuracy in a geolocation system [3].

C. Effects of Time Diversity

Here, we study the effects of time diversity with the two diversity combining schemes, i.e., GDCS and CMDCS, that we discussed in Section IV. Time diversity is simulated by running simulations using the four measurements of each location, collected consecutively while stopping movement in the vicinity of the transmitter and the receiver antennas during the measurement. This represents the situation in which the system is used for quasistationary applications with four time-diversity branches. Fig. 10 presents simulation results for the EV/FBCM method with two diversity-combining schemes, i.e., EV/FBCM/TD4-CMDCS and EV/FBCM/TD-GDCS. Simulation results for the EV/FBCM method without time diversity are also shown in the figure as a reference for comparison. From the results, we can observe that there is almost no difference between the performances of the CMDCS-based method and the nondiversity method while the GDCS-based

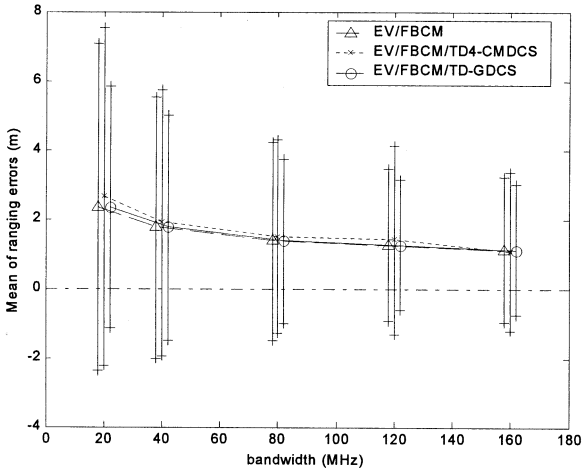

Fig. 10. Mean and STD of ranging errors with time diversity.

method has clearly better performance in terms of smaller STD of ranging errors. This verifies our earlier comment that the CMDCS is not suitable for time-diversity systems. In contrast, GDCS can be used in time-diversity systems to improve the system statistical performance to some extent.

D. Effects of Frequency Diversity

The use of frequency diversity is simulated by running simulations based on segments of data samples that are obtained by dividing each measurement data sequence of frequency channel response into a number of equally spaced segments. Since the measurement data at each location are of 200-MHz bandwidth, to avoid overlapping among diversity segments, the effect of frequency diversity is evaluated only for a bandwidth of 20 MHz. It should be noted that in real implementation, overlapping segments can be used for frequency diversity. In our simulations, the overlapping is avoided in order to avoid correlation between measurement noises in the overlapping segments since the segments are obtained from one measurement. Four equally spaced segments are first used for each measurement data sequence to compare frequency and time-diversity techniques using the same number of diversity branches. Both GDCS and CMDCS schemes are used for EV/FBCM (i.e., EV/FBCM/FD4-GDCS and EV/FBCM/FD4-CMDCS), and the results are compared with that of EV/FBCM and EV/FBCM/TD-GDCS, as shown in Fig. 11(a). The cumulative distribution function (CDF) is used for comparison. From the figure, we note that all three diversity techniques perform better than the nondiversity EV/FBCM method and frequency diversity with CMDCS has the best performance. In order to examine the effects of the number of diversity branches, we increase the number of diversity branches to ten, which is the maximum number of segments that we can achieve from 200-MHz measurement data without overlapping segments. Then, in Fig. 11(b), the simulation results of GDCS and CMDCS schemes with ten diversity branches (i.e., EV/FBCM/FD10-GDCS and EV/FBCM/FD10-CMDCS) are compared with that of nondiversity EV/FBCM and frequency diversity with four diversity branches, i.e., EV/FBCM/FD4-CMDCS, which has the best

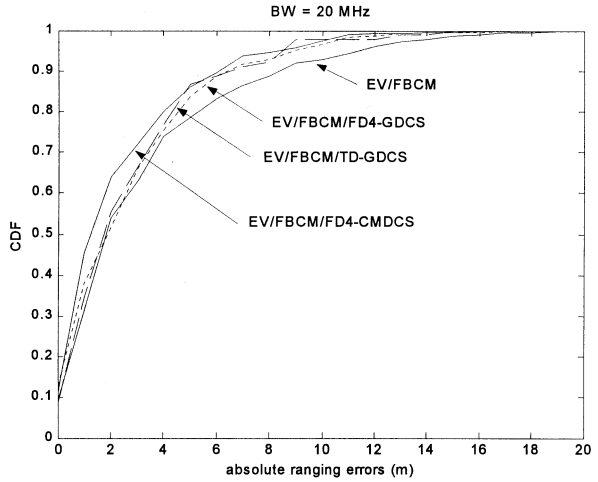

(a)

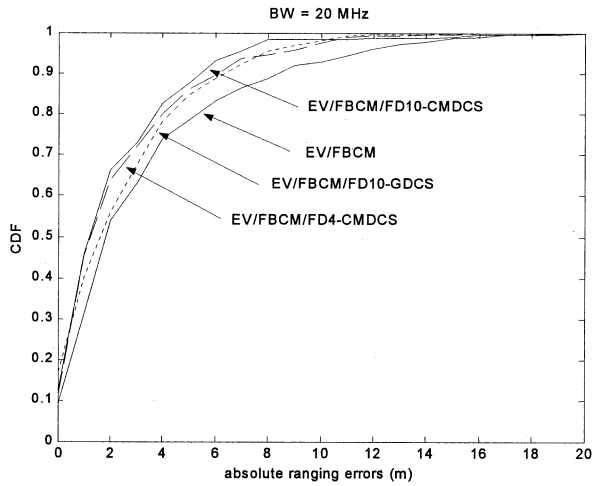

(b)

Fig. 11. CDF of ranging errors for a bandwidth of 20 MHz with frequency diversity.

performance in Fig. 11(a). From the results, it is clear that EV/FBCM/FD10-CMDCS has the best performance and even the EV/FBCM/FD4-CMDCS has slightly better performance than EV/FBCM/FD10-GDCS, though it has a smaller number of diversity branches. Consequently, we can conclude that frequency diversity can further improve the ranging performance and for frequency diversity, the CMDCS scheme is preferred to the GDCS.

VI. Conclusion

In this paper, we have applied super-resolution spectral estimation techniques to the measured channel frequency response to accurately estimate TOA for indoor geolocation applications. Our results show that super-resolution techniques can significantly improve the performance of TOA estimation as compared with conventional techniques including direct IFT and DSSS signal-based cross-correlation techniques. We have shown that a number of techniques are able to further improve the performance of super-resolution techniques, including the EV method, forward–backward estimation of correlation matrix, time diversity, and frequency diversity. For time diversity, the general diversity combining scheme is preferred while for frequency diversity, the correlation matrix-based scheme is preferred. Another important factor that affects the performance of TOA estimation is signal bandwidth. For all techniques the performance improves as signal bandwidth increases. On the other hand, as bandwidth increases, there is less difference in performance between different techniques. Also, it should be noted that due to the possibility of the NLOS condition between transmitter and receiver, using super-resolution techniques and large bandwidth cannot eliminate large ranging errors at some locations.

Appendix

The parameter correlation matrix is defined in (6) as

$$\mathbf{A} = E\{\mathbf{a}\mathbf{a}^H\}. \tag{A1}$$

Thus, using the forward estimation method, the (i,j)th element of the correlation matrix $\mathbf{A}$ can be obtained as

$$\begin{aligned} A_{ij} &= E\{\alpha_i' \alpha_j'^*\} \\ &= \frac{1}{M}\sum_{k=0}^{M-1} (\alpha_i e^{-j2\pi(f_0+k\Delta f)\tau_i}) \times (\alpha_j e^{-j2\pi(f_0+k\Delta f)\tau_{ji}})^* \\ &= \frac{1}{M}\alpha_i\alpha_j^* e^{-j2\pi f_0(\tau_i-\tau_j)} \sum_{k=0}^{M-1} e^{-j2\pi k\Delta f(\tau_i-\tau_j)} \\ &= \frac{1}{M}\alpha_i\alpha_j^* e^{-j2\pi f_0(\tau_i-\tau_j)} \frac{1-e^{-j2\pi M\Delta f(\tau_i-\tau_j)}}{1-e^{-j2\pi\Delta f(\tau_i-\tau_j)}} \\ &= \alpha_i\alpha_j^* e^{-j2\pi f_0(\tau_i-\tau_j)} e^{-j\pi(M-1)\Delta f(\tau_i-\tau_j)} \\ &\quad \times \frac{\sin[M\pi\Delta f(\tau_i-\tau_j)]}{M\sin[\pi\Delta f(\tau_i-\tau_j)]} \end{aligned} \tag{A2}$$

and it easily follows that

$$A_{ii} = |\alpha_i|^2 \tag{A3}$$

where $\alpha_i = |\alpha_i| e^{j\theta_i}$. From the definition of the correlation coefficient between the ith and jth parameters, defined as in [18], we can obtain that

$$\rho_{ij}^{(\mathrm{FCM})} = \frac{A_{ij}}{\sqrt{A_{ii}A_{jj}}} = Ke^{-j\phi} \tag{A4}$$

where K and ϕ are defined in (13).

The FBCM is defined in (12)

$$\hat{\mathbf{R}}_{xx}^{(\mathrm{FB})} = \frac{1}{2}(\hat{\mathbf{R}}_{xx} + \mathbf{J}\hat{\mathbf{R}}_{xx}^*\mathbf{J}) \tag{A5}$$

where $\hat{\mathbf{R}}_{xx}$ and $\mathbf{J}\hat{\mathbf{R}}_{xx}^*\mathbf{J}$ are forward and backward correlation matrices, respectively. The backward correlation matrix can be equivalently calculated using (11) with the data vector

$$\mathbf{x} = [\,x(L-1) \quad x(L-2) \quad \ldots \quad x(0)\,]^H \tag{A6}$$

so that the element of the parameter vector $\mathbf{a}$ in (5) becomes

$$\alpha_k' = \alpha_k^* e^{j2\pi(f_0+(L-1)\Delta f)\tau_k}. \tag{A7}$$

Thus, using the backward estimation method, the (i,j)th element of the parameter correlation matrix can be obtained as (A8), shown at the top of the page, where A_{ij} is given by (A2). Then, the (i,j)th element of the parameter correlation matrix using the forward–backward estimation method can be obtained as

$$A_{ij}^{(\mathrm{FB})} = \frac{1}{2}\left(A_{ij} + A_{ij}^{(\mathrm{B})}\right). \tag{A9}$$

$$
\begin{aligned}
A_{ij}^{(\mathrm{B})} &= \frac{1}{M}\sum_{k=0}^{M-1}\left(\alpha_i^* e^{j2\pi(f_0+k\Delta f+(L-1)\Delta f)\tau_i}\right)\times\left(\alpha_j^* e^{j2\pi(f_0+k\Delta f+(L-1)\Delta f)\tau_{ji}}\right)^* \\
&= \frac{1}{M}\alpha_i^*\alpha_j e^{j2\pi(f_0+(L-1)\Delta f)(\tau_i-\tau_j)}\sum_{k=0}^{M-1} e^{j2\pi k\Delta f(\tau_i-\tau_j)} \\
&= \frac{1}{M}\alpha_i^*\alpha_j e^{j2\pi(f_0+(L-1)\Delta f)(\tau_i-\tau_j)}\frac{1-e^{j2\pi M\Delta f(\tau_i-\tau_j)}}{1-e^{j2\pi\Delta f(\tau_i-\tau_j)}} \\
&= \alpha_i^*\alpha_j e^{j2\pi(f_0+(L-1)\Delta f)(\tau_i-\tau_j)} e^{j\pi(M-1)\Delta f(\tau_i-\tau_j)}\frac{\sin[M\pi\Delta f(\tau_i-\tau_j)]}{M\sin[\pi\Delta f(\tau_i-\tau_j)]} \\
&= A_{ij}^* e^{j2\pi(L-1)\Delta f(\tau_i-\tau_j)} \qquad \text{(A8)}
\end{aligned}
$$

Finally, the correlation coefficient between the ith and jth parameters can determined by

$$
\begin{aligned}
\rho_{ij}^{(\mathrm{FBCM})} &= \frac{A_{ij}^{(\mathrm{FB})}}{|\alpha_i||\alpha_j|} \\
&= \frac{1}{2}\left(Ke^{-j\phi}+Ke^{j(\phi+\psi)}\right) \\
&= K\cos\left(\phi+\frac{\psi}{2}\right)e^{j\psi/2} \qquad \text{(A10)}
\end{aligned}
$$

where ψ is given in (14).

For frequency diversity, we assume the carrier frequency is uniformly distributed as given in (19). The elements of the parameter correlation matrix are derived as follows:

$$
\begin{aligned}
A_{ij}^{(\mathrm{FD})} &= E\{\alpha_i'\alpha_j'^*\} \\
&= \frac{1}{\Delta F}\int_{f_c-\Delta F/2}^{f_c+\Delta F/2}\alpha_i\alpha_j^* e^{-j2\pi f_0(\tau_i-\tau_j)}df_0 \\
&= \alpha_i\alpha_j^* e^{-j2\pi f_c(\tau_i-\tau_j)}\frac{\sin[\pi\Delta F(\tau_i-\tau_j)]}{\pi\Delta F(\tau_i-\tau_j)} \qquad \text{(A11)}
\end{aligned}
$$

and the correlation coefficient is easily obtained

$$
\begin{aligned}
\rho_{ij}^{(\mathrm{FD})} &= \frac{A_{ij}^{(\mathrm{FD})}}{|\alpha_i||\alpha_j|} \\
&= \frac{\sin(\pi\Delta F(\tau_i-\tau_j))}{\pi\Delta F(\tau_i-\tau_j)}e^{j[(\theta_i-\theta_j)-2\pi f_c(\tau_i-\tau_j)]}. \qquad \text{(A12)}
\end{aligned}
$$

The correlation coefficients of forward and forward–backward estimation methods, given in (21) and (22), are easily obtained by noticing that

$$
\begin{aligned}
\rho_{ij}^{(\mathrm{FCM,FD})} &= E\left\{\rho_{ij}^{(\mathrm{FCM})}\right\} \\
\rho_{ij}^{(\mathrm{FBCM,FD})} &= E\left\{\rho_{ij}^{(\mathrm{FBCM})}\right\} \qquad \text{(A13)}
\end{aligned}
$$

where the statistical expectation $E\{\cdot\}$ is performed with respect to the uniformly distributed carrier frequency.

ACKNOWLEDGMENT

The authors would like to thank members of the CWINS at WPI, who have contributed in various ways to this work. In particular, they would like to thank Dr. J. Beneat and Dr. P. Krishnamurthy, for their work in building the database of channel measurements that were used in this paper, and Dr. A. Levesque and Dr. R. Tingley, for their comprehensive reviews that have greatly improved the manuscript.

REFERENCES

[1] K. Pahlavan and P. Krishnamurthy, *Principles of Wireless Networks—A Unified Approach*. Englewood Cliffs, NJ: Prentice-Hall, 2002.
[2] K. Pahlavan, P. Krishnamurthy, and J. Beneat, "Wideband radio propagation modeling for indoor geolocation applications," *IEEE Commun. Mag.*, vol. 36, pp. 60–65, Apr. 1998.
[3] K. Pahlavan, X. Li, and J. Makela, "Indoor geolocation science and technology," *IEEE Commun. Mag.*, vol. 40, pp. 112–118, Feb. 2002.
[4] D. Manolakis, V. Ingle, and S. Kogon, *Statistical and Adaptive Signal Processing*. New York: McGraw-Hill, 2000.
[5] W. Beyene, "Improving time-domain measurements with a network analyzer using a robust rational interpolation technique," *IEEE Trans. Microwave Theory Tech.*, vol. 49, pp. 500–508, Mar. 2001.
[6] H. Yamada, M. Ohmiya, Y. Ogawa, and K. Itoh, "Superresolution techniques for time-domain measurements with a network analyzer," *IEEE Trans. Antennas Propagat.*, vol. 39, pp. 177–183, Feb. 1991.
[7] T. Lo, J. Litva, and H. Leung, "A new approach for estimating indoor radio propagation characteristics," *IEEE Trans. Antennas Propagat.*, vol. 42, pp. 1369–1376, Oct. 1994.
[8] G. Morrison and M. Fattouche, "Super-resolution modeling of the indoor radio propagation channel," *IEEE Trans. Veh. Technol.*, vol. 47, pp. 649–657, May 1998.
[9] M. Pallas and G. Jourdain, "Active high resolution time delay estimation for large BT signals," *IEEE Trans. Signal Processing*, vol. 39, pp. 781–788, Apr. 1991.
[10] L. Dumont, M. Fattouche, and G. Morrison, "Super-resolution of multipath channels in a spread spectrum location system," *Electron. Lett.*, vol. 30, pp. 1583–1584, Sept. 1994.
[11] H. Saarnisaari, "TLS-ESPRIT in a time delay estimation," in *Proc. IEEE 47th VTC*, 1997, pp. 1619–1623.
[12] Saleh and R. Valenzuela, "A statistical model for indoor multipath propagation," *IEEE J. Select. Areas Commun.*, vol. SAC-5, pp. 128–137, Feb. 1987.
[13] K. Pahlavan and A. Levesque, *Wireless Information Networks*. New York: Wiley, 1995.
[14] G. Yang, "Performance evaluation of high speed wireless data systems using a 3D ray tracing algorithm," Ph.D. dissertation, Worcester Polytech. Inst., Worcester, MA, 1994.
[15] S. Howard and K. Pahlavan, "Measurement and analysis of the indoor radio channel in the frequency domain," *IEEE Trans. Instrum. Meas.*, vol. 39, pp. 751–755, Oct. 1990.
[16] R. Schmidt, "A signal subspace approach to multiple emitter location and spectral estimation," Ph.D. dissertation, Stanford Univ., Stanford, CA, 1981.
[17] R. Williams, S. Prasad, A. Mahalanabis, and L. Sibul, "An improved spatial smoothing technique for bearing estimation in a multipath environment," *IEEE Trans. Acoust., Speech, Signal Processing*, vol. 36, pp. 425–432, Apr. 1988.
[18] V. Reddy, A. Paulraj, and T. Kailath, "Performance analysis of the optimum beamformer in the presence of correlated sources and its behavior under spatial smoothing," *IEEE Trans. Acoust., Speech, Signal Processing*, vol. ASSP-35, pp. 927–936, July 1987.
[19] D. Tufts and R. Kumaresan, "Estimation of frequencies of multiple sinusoids: Making linear prediction perform like maximum likelihood," *Proc. IEEE*, vol. 70, pp. 975–989, Sept. 1982.
[20] H. Krim and M. Viberg, "Two decades of array signal processing research," *IEEE Signal Processing Mag.*, vol. 13, pp. 67–94, July 1996.

[21] J. Liberti and T. Rappaport, *Smart Antennas for Wireless Communications: IS-95 and Third Generation CDMA Applications*. Englewood Cliffs, NJ: Prentice-Hall, 1999.
[22] S. Lang and J. Mclellan, "Frequency estimation with maximum entropy spectral estimators," *IEEE Trans. Acoust., Speech, Signal Processing*, vol. ASSP-28, pp. 716–724, Dec. 1980.
[23] M. Wax and T. Kailath, "Detection of signals by information theoretic criteria," *IEEE Trans. Acoust., Speech, Signal Processing*, vol. ASSP-33, pp. 387–392, Apr. 1985.
[24] G. Xu, R. Roy, and T. Kailath, "Detection of number of sources via exploitation of centro-symmetry property," *IEEE Trans. Signal Processing*, vol. 42, pp. 102–112, Jan. 1994.
[25] D. Johnson and S. DeGraaf, "Improving the resolution of bearing in passive sonar arrays by eigenvalue analysis," *IEEE Trans. Acoust., Speech, Signal Processing*, vol. ASSP-30, pp. 638–647, Aug. 1982.
[26] T. Rappaport, *Wireless Communications Principles and Practice*. Englewood Cliffs, NJ: Prentice-Hall, 1996.
[27] S. Howard and K. Pahlavan, "Autoregressive modeling of wide-band indoor radio propagation," *IEEE Trans. Commun.*, vol. 40, pp. 1540–1552, Sept. 1992.
[28] J. Beneat, K. Pahlavan, and P. Krishnamurthy, "Radio channel characterization for geolocation at 1 GHz, 500 GHz, 90 MHz and 60 MHz in SUO/SAS," in *Proc. IEEE MILCOM*, 1999, pp. 1060–1063.
[29] B. Ulriksson, "Conversion of frequency-domain data to the time domain," *Proc. IEEE*, vol. 74, pp. 74–76, Jan. 1986.

Xinrong Li (S'00) received the B.E. degree from the University of Science and Technology of China, Hefei, China, in 1995 and the M.E. degree from the National University of Singapore, in 1999. He is currently pursuing the Ph.D. degree in wireless communications and networks at the Worcester Polytechnic Institute (WPI), Worcester, MA.

From 1995 to 1997, he was a System Engineer at the Shenyang Institute of Automation, Chinese Academy of Sciences, Shenyang, China. Since 1999, he has been working as a Research Assistant at the Center for Wireless Information Network Studies, WPI, on various research projects sponsored by Nokia, TEKES, Sonera, United Technologies Research Center, and the National Science Foundation. During the summer of 2002, he worked on system capacity and performance measurement and analysis of 3G all-IP CDMA2000 1xEV-DO Network Infrastructure Systems at Airvana, Inc., Chelmsford, MA. His research interests include statistical signal processing, indoor geolocation, performance analysis of wireless communication and network systems, and measurement and modeling of indoor radio propagation channels.

Kaveh Pahlavan (M'79–SM'88–F'96) is a Professor of Electrical and Computer Engineering, a Professor of Computer Science, and Director of the Center for Wireless Information Network Studies, Worcester Polytechnic Institute, Worcester, MA. He is also a Visiting Professor of the Telecommunication Laboratory and the Centre for Wireless Communications (CWC), University of Oulu, Oulu, Finland. His area of research is broadband wireless indoor networks. He has contributed to numerous seminal technical publications in this field. He is the principal author (with A. Levesque) of the *Wireless Information Networks* (New York: Wiley, 1995) and (with P. Krishnamurthy) *Principles of Wireless Networks–A Unified Approach* (Englewood Cliffs, NJ: Prentice-Hall, 2002). He has been a consultant to a number of companies including CNR Inc, GTE Laboratories, Steinbrecher Co., Simplex, Mercury Computers, WINDATA, SieraComm, 3COM, and Codex/Motorola in MA; JPL, Savi Technologies, RadioLAN in CA; Aironet in OH; United Technology Research Center in CT; Honeywell in AZ; Nokia, LK-Products, Elektrobit, TEKES, and Finnish Academy in Finland; and NTT in Japan. Before joining WPI, he was the Director of Advanced Development at Infinite Inc., Andover, MA, working on data communications. He started his career as an Assistant Professor at Northeastern University, Boston, MA.

He is the Editor-in-Chief of the *International Journal on Wireless Information Networks*. He was the Founder, Program Chairman, and Organizer of the IEEE Wireless LAN Workshop, Worcester, MA, in 1991 and 1996, and the Organizer and Technical Program Chairman of the IEEE International Symposium on Personal, Indoor, and Mobile Radio Communications (PIMRC), Boston, MA, in 1992 and 1998. He was selected as a member of the Committee on Evolution of Untethered Communication, U.S. National Research Council, in 1997 and has led the U.S. review team for the Finnish Research and Development Programs in Electronic and Telecommunication, in 1999. For his contributions to the wireless networks, he was the Westin Hadden Professor of Electrical and Computer Engineering at Worcester Polytechnic Institute from 1993 to 1996 and become a fellow of Nokia in 1999. From May of 2000, he was the first Fulbright-Nokia scholar at the University of Oulu. Because of his inspiring visionary publications and his international conference activities for the growth of the wireless LAN industry, he is referred to as one of the founding fathers of the wireless LAN industry. Details of his contributions to this field are available at www.cwins.wpi.edu.